Preparation and Thermal Property of Hybrid Nanocomposites by Free Radical Copolymerization of Styrene with Octavinyl Polyhedral Oligomeric Silsesquioxane

Benhong Yang,[1,2] Hongyao Xu,[1,3] Jiafeng Wang,[1] Shanyi Gang,[3] Cun Li[1]

[1]*School of Chemistry and Chemical Engineering, Anhui University, Hefei 230039, People's Republic of China*
[2]*Department of Chemical and Material Engineering, Hefei University, Hefei 230022, People's Republic of China*
[3]*College of Material Science and Engineering and State Key Laboratory for Modification of Chemical Fibers and Polymeric Materials, Dong Hua University, Shanghai 200051, People's Republic of China*

ABSTRACT: The poly(styrene-*co*-octavinyl-polyhedral oligomeric silsesquioxane) (PS–POSS) organic–inorganic hybrid nanocomposites containing various percent of POSS were prepared via one-step free radical polymerization and characterized by FTIR, high-resolution ^{1}H NMR, ^{29}Si NMR, GPC, DSC, and TGA technologies. The POSS contents in these nanocomposites were determined using FTIR calibration curve. The result shows that the POSS contents in nanocomposites can be tailored by varying the POSS feed ratios. On the basis of the POSS contents in the nanocomposites and the ^{1}H NMR spectra, the number of reacted vinyl groups of each octavinyl-POSS macromonomer were calculated to be 6–8.

DSC and TGA measurements indicate that the incorporation of POSS into PS homopolymer can apparently improve the thermal properties of the polymeric materials. The dramatic T_g and T_{dec} increases are mainly due to the formation of star and low cross-linking structure of the nanocomposites, where POSS cores behave as the joint points and hinder the motion and degradation of the polymeric chains. © 2007 Wiley Periodicals, Inc. J Appl Polym Sci 106: 320–326, 2007

Key words: synthesis; nanocomposites; free radical polymerization; thermal properties; polyhedral oligomeric silsesquioxane

INTRODUCTION

Polymeric materials have undergone extensive applications in our daily lives because of their good processability and low cost. However, the absence of excellent thermal stability is an inherent drawback of polymeric materials. A good method to improve thermal properties of polymeric materials is to develop organic–inorganic hybrid composites that combine the properties of traditional organic polymers (i.e., processability, toughness, low cost) with the properties of inorganic compounds (i.e. thermal and oxidative stability). A well studied class of materials is clay nanocomposites, where the included clay has one major dimension on the size scale of 1–100 nm.[1–5]

Polyhedral oligomeric silsesquioxane (POSS) is a type of nanoscale molecule that has a well-defined cube-like inorganic core (Si_8O_{12}) with its corners connected with eight organic functional groups (reactive or inert).[6] Since the number and type of the functional groups on POSS cages can be readily varied, POSS molecules are excellent nanobuilding blocks for preparing various organic–inorganic hybrid nanocomposites with variety of structures such as linear, branched, star-shaped as well as network types. In these hybrid nanocomposites, POSS moieties are chemically bonded and homogeneously dispersed in the polymeric systems, and thus largely enhance the thermal and mechanical properties of these hybrid materials. So far, most researches on POSS-containing polymeric systems have been directed toward the linear or pendent nanocomposites by using POSS macromonomers with one or two functional organic groups. These studied nanocomposites include poly(styrene-*co*-POSS),[7] poly(acrylate-*co*-POSS),[8,9] poly(norbornene-*co*-POSS),[10] poly(vinylpyrrolidone-*co*-POSS),[11,12] poly(ethylene-*co*-POSS),[13,14] poly(epoxy-*co*-POSS),[15] poly(butadiene-*co*-POSS),[16] poly(urethane-*co*-POSS),[17,18] poly(acetoxystyrene-*co*-POSS),[19] poly(siloxane-*co*-POSS),[20,21] and so on.

Multifunctional POSS monomers with more than two functional organic groups are perfect structure-guiding agents for the synthesis of star-shaped or network nanocomposites. Therefore, some pioneer researchers are shifting their interests toward this

---

area, and many efforts have been made so far.[22–32] However, these works were mainly involving the preparation of these hybrid nanocomposites, and properties of the nanocomposites were little discussed.[33] In this study, we report the syntheses and characterization of a series of soluble PS–POSS hybrid nanocomposites from styrene and octavinyl-polyhedral oligomeric silsesquioxane using common free radical polymerization technique. The thermal properties of the nanocomposites were studied by DSC and TGA technologies and the T_g increase mechanism was specially discussed.

EXPERIMENTAL

Materials

Styrene was purchased from Shanghai Reagent Co., China and distilled from hydroquinone under reduced pressure, and then stored in sealed ampoules in a refrigerator. Azobis(isobutyronitrile) (AIBN) was obtained from Shanghai Reagent Co. and refined in heated ethanol and kept in a dried box. Spectroscopic-grade THF and 1,4-dioxane were dried over 4 Å molecular sieves and distilled from sodium benzophenone ketyl immediately prior to use. All other solvents were used without further purification.

Instrumentation analyses

The FTIR spectra were measured with a spectral resolution of 1 cm^{-1} on a Nicolet NEXUS 870 FTIR spectrophotometer using KBr powder at room temperature. ^{1}H NMR spectra were recorded on a Bruker AVANCE/DMX 300 spectrometer using chloroform-d solvent. High-resolution ^{29}Si NMR spectra were carried out at room temperature using a Bruker DSX-400 spectrometer operating at resonance frequency of 79.49 MHz. Weight-average (M_w) and number-average (M_n) molecular weights and polydispersity index (PDI, M_w/M_n) were determined by a Waters 515 gel permeation chromatograph (GPC). Differential scanning calorimetry (DSC) was performed on a TA Instruments DSC 9000 equipped with a liquid nitrogen cooling accessory (LNCA) unit under a continuous nitrogen purge (50 mL/min). The scan rate was 20°C/min at the temperature range of 20–250°C. Samples were quickly cooled to 0°C from the melt for the first scan and then scanned from 20 to 250°C at 10°C/ min. The glass transition temperature (T_g) was taken as the midpoint of the specific heat increment. Thermogravimetric analyses were carried out using a TA Instruments TGA 2050 thermogravimetric analyzer with a heating rate of 10°C/min from 25 to 550°C under a continuous nitrogen purge (100 mL/min). The thermal degradation temperature (T_{dec}) was defined as the temperature of 5% weight lost.

Syntheses of monomers and polymers

Octavinyl-polyhedral oligomeric silsesquioxane

Octavinyl-polyhedral oligomeric silsesquioxane (Octavinyl-POSS) was synthesized in our laboratory according to the procedures described in Ref. 34. Typically, vinyltriethoxysilane (10.5 mL, 0.05 mol) was dissolved in 24.5 mL of anhydrous ethanol with stirring and then some amount of hydrochloric acid and 3 mL of water were added to adjust solution to pH 3. The system was allowed to react for 10 h at 60°C under N$_2$. The mixture was cooled down to room temperature. The white crystalline powder was filtered, washed with cyclohexane and recrystallized from tetrahydrofuran/methanol (1:3) to give 0.72 g (18.2%).

FTIR (KBr, ν, cm^{-1}): 1605 (CH=CH), 1414, 1273 (C-H), 1100 (Si-O-Si);

^{1}H-NMR: (CDCl$_3$, ppm) 5.58 (HHC=CH^b, 8H, dd, $J = 12.4$ and $J = 15.0$ Hz), 6.01 (H$H^{a'}$C=CH, 8H, dd, $J = 2.4$ and $J = 12.4$ Hz), 6.10 (H^a$H^{a'}$C=CH, 8H dd, $J = 2.4$ and $J = 15.0$ Hz).

Hybrid nanocomposite

All polymerization reactions were carried out under nitrogen atmosphere using a standard Schlenk vacuum-line system. For comparison, the homopolystyrene (PS) was also synthesized. In a typical reaction, 9.62 mmol of styrene and 0.08 mmol of POSS monomer in 5 mL of dried 1,4-dioxane were added in a three-necked flask stirred for 8 h at 70°C under a nitrogen atmosphere, using the AIBN initiator (1 wt % on the basis of monomer). The crude product was added dropwise into excessive ethanol at 60°C under vigorously agitation to dissolve the unreacted monomers and precipitate the nanocomposite. The product was redissolved in THF to form a homogeneous and transparent solution, and then precipitated in ethanol. This purification procedure was repeated twice to ensure thorough removal of the POSS and styrene from PS–POSS nanocomposite, and finally the product was dried in a vacuum oven. A 41 wt % yield was obtained through this procedure.

HF-treated samples for GPC analysis

The organic chains connected on or between POSS cages were prepared by dissolving the silica core (POSS) with HF and extracted for GPC analyses. In a typical procedure, 0.05 g of the PS–POSS nanocomposite was dissolved in 5 mL of THF in a polytetrafluoroethylene bottle. About 0.05 mL of 50% HF was dropped into the solution, and the mixture was kept at room temperature for 72 h. Then, THF was removed by rotary evaporation. The residual material was mixed with freshly dried ether to extract the or-
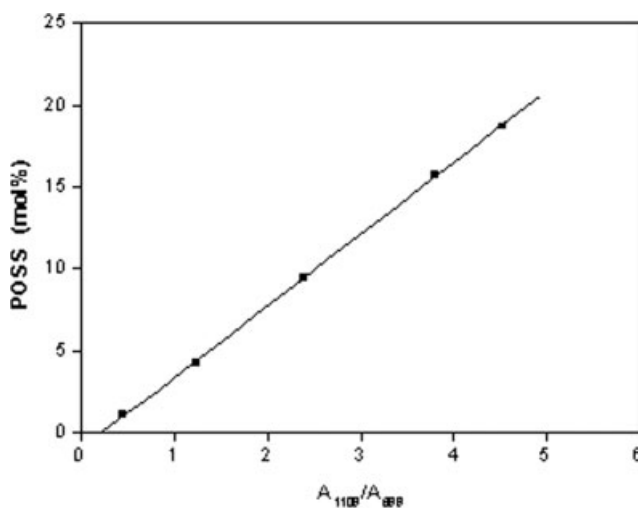
Figure 1 IR calibration curve for determining POSS contents in PS–POSS nanocomposites.

ganic components. The extracted solution was filtered and ether in the filtrate solution was removed. A viscous liquid was obtained and dissolved in 1 mL of THF for GPC analysis.

POSS content determination[35]

The FTIR technology was employed to determine the POSS contents in the PS–POSS nanocomposites. On the IR spectra, the PS shows a characteristic absorption band at 699 cm^{-1}, where POSS has no absorption band, and the POSS has an absorption band at $\sim$ 1109 cm^{-1}, where PS does not display any absorption. Thus the POSS contents in the PS–POSS nanocomposites can be estimated by the calibration curve method. A series of PS/POSS mixtures with different POSS contents were first dissolved in THF to ensure intimate mixing and then cast into thin films for FTIR testing. The calibration curve of A_{1109}/A_{699} against POSS molar contents in the mixtures is plotted (shown in Fig. 1), and the linear relationship between POSS molar percentage (Y_{POSS}) and A_{1109}/A_{699} is showed and expressed as Formula 1.

$$Y_{poss} = 0.044(A_{1109}/A_{699}) - 0.0094 \qquad (1)$$

RESULTS AND DISCUSSION

Polymerization and structure characterization

The PS–POSS nanocomposites were prepared by the free radical polymerization technique as shown in Scheme 1. For comparison, the homopolystyrene (PS) was also synthesized. Figure 2 shows the FTIR spectra of pure POSS, PS, and PS–POSS. The pure POSS shows a characteristic Si-O-Si stretching absorption
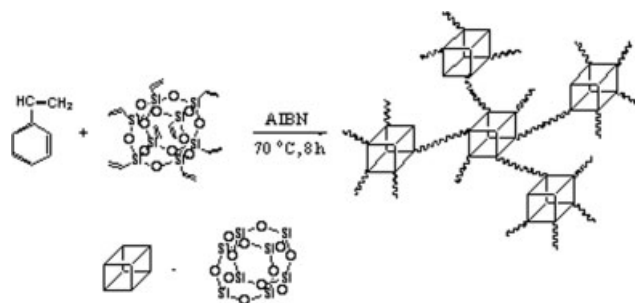
Scheme 1 Formation of PS–POSS nanocomposites via free radical polymerization.

band at $\sim$ 1109 cm^1. The PS shows two characteristic out-of-plane wagging absorption bands of single-substituted aromatic ring at 699 and 756 cm^{-1}. The peaks at $\sim$ 1500 cm^{-1} are assigned to the skeletal vibration of aromatic ring. The stretching absorption bands of methylene and methine groups are located at $\sim$ 2900 cm^{-1}. The spectra of all PS–POSS nanocomposites are similar to that of the PS, except that a strong and symmetric peak appears at $\sim$ 1109 cm^{-1} in all the spectra, which is the characteristic Si-O-Si stretching of silsesquioxane cages. And meanwhile, we found that the intensity of this vibration absorption increases with the POSS feed ratio, indicating that the POSS cage may have been incorporated into the polymeric chains.

By detecting the A_{1109}/A_{699} values of the PS–POSS nanocomposites, the POSS molar contents in the hybrid nanocomposites were determined on the basis of the calibration curve (Fig. 1), and the results are shown in Table I. Table I shows that the molar content of the POSS in the nanocomposites increases with the increase of POSS feed ratio, indicating that the
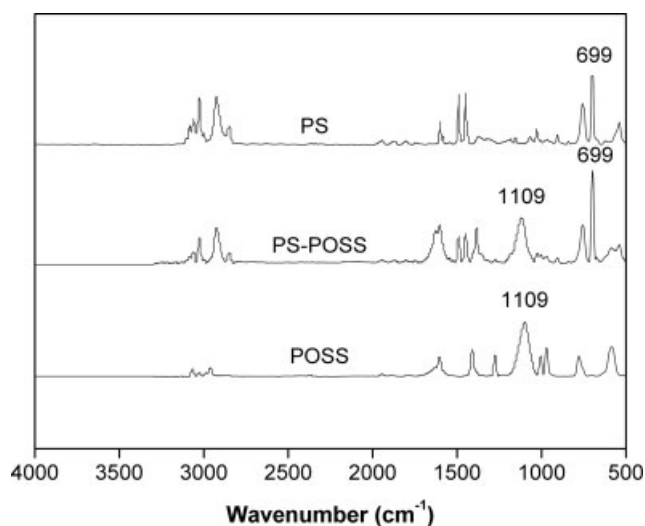

Figure 2 FTIR spectra of pure POSS, PS, and PS–POSS nanocomposites.

TABLE I
Effect of POSS Feed Ratio on the Properties of PS–POSS Nanocomposites

| No | POSS (mol %) | | Yield (wt %) | M_w[b] ($\times 10^3$ g/mol) | M_n ($\times 10^3$ g/mol) | PDI | x[c] | T_g[d] | T_{dec}[e] | Char yield (%) |
	Feed mole ratio	Product mole ratio[a]								
1	0.00	0.00	45.2	12.8	6.81	1.88	–	92.4	313.2	0
2	0.17	0.08	43.1	10.0	6.38	1.43	8.0	94.5	307.5	0
3	0.81	0.37	39.3	12.3	7.87	1.44	7.3	97.3	334.9	1
4	1.46	1.21	39.1	11.6	7.63	1.52	6.9	99.6	336.9	3
5	2.41	1.45	38.6	10.5	6.27	1.68	6.7	104.1	339.2	4
6	3.18	2.21	37.1	12.6	8.63	1.46	5.8	107.4	348.1	4

[a] Data were obtained based on the IR standard curve.
[b] Data were determined by GPC using the PS standard curve.
[c] Number of reacted vinyl groups on POSS macromonomer.
[d] Data were gathered on the second melt using a heating rate of 10°C/min.
[e] Data were taken to be the temperature at 5% weight loss.

content of POSS in the nanocomposites can be effectively adjusted by varying POSS feed ratio.

Figure 3 shows ^{1}H NMR spectra of POSS, PS and PS–POSS in d-chloroform solvent. For the pure POSS macromonomer, the resonance band of vinyl protons is observed at ~ 6.0 ppm as multiple peaks because of the coupling of hydrogen protons. For homopolymer PS, the broad resonance bands at 7.1 and 6.6 ppm are attributed to the aromatic protons. The peaks of the methine protons and methylene protons are at 1.8 and 1.4 ppm, respectively. The PS–POSS shows a similar spectrum to that of the pure PS. It also exhibits resonance peaks at 7.1, 6.6, 1.8, and 1.4 ppm, respectively. Besides, there is a wide resonance band at nearby 6 ppm, which belongs to the unreacted vinyl protons of POSS molecules, indicating that not all the vinyl groups of POSS have participated in the copolymerization. Since the resonance bands of methine and methylene protons from the POSS moiety overlap with those from the PS chains, the average number of the reacted vinyl groups (x) of each POSS cage can be calculated on the basis of Formula (2) (when $x < 7$) or Formula (3) (when $x \geq 7$).

$$\text{POSS}(mol)\% = \frac{\frac{A_{6.0}}{3(8-x)}}{\frac{A_{6.0}}{3(8-x)} + \frac{A_{6.6}+A_{7.1}}{5}} \times 100 \qquad (2)$$

$$\text{POSS}(mol)\% = \frac{\frac{A_{1.8}+A_{1.4}}{3} - \frac{A_{6.6}+A_{7.1}}{5}}{\frac{A_{1.8}+A_{1.4}}{3} - \frac{A_{6.6}+A_{7.1}}{5} + \frac{x(A_{6.6}+A_{7.1})}{5}} \times 100 \qquad (3)$$

In Formulae (2) and (3), POSS (mol)% is the POSS molar content detected by the IR method. $A_{1.4}$, $A_{1.8}$, $A_{6.0}$, $A_{6.6}$, and $A_{7.1}$ are the integral areas of the resonance peaks at 1.4, 1.8, 6.0, 6.6, 7.1 ppm, respectively, which are obtained from the ^{1}H NMR spectra. The x value of each resulting PS–POSS nanocomposite was calculated and shown in Table I, which reveals that

6–8 vinyl groups of each POSS molecule have participated in the copolymerization with styrene to form hybrid nanocomposites.

The high-resolution ^{29}Si NMR spectroscopy provides further insight to the copolymerization of styrene with the POSS macromonomers. Figure 4 shows the ^{29}Si NMR spectra of both pure POSS macromonomer and PS–POSS nanocomposite (2.21 mol % POSS). For pure octavinyl-POSS, there is only one resonance peak at -79.5 ppm, because all silicon atoms have the same chemical environment in the POSS cages. The nanocomposite shows two resonance bands at -65.5 and -79.8 ppm, respectively referring to the silicon atoms connected to the reacted and the unreacted vinyl groups on the POSS cages. Since the peak area at -65.5 ppm is much bigger than that at -79.8 ppm, we think that most vinyl groups of each POSS molecule have participated in the copolymerization with styrene to form hybrid nanocomposites. This sup-
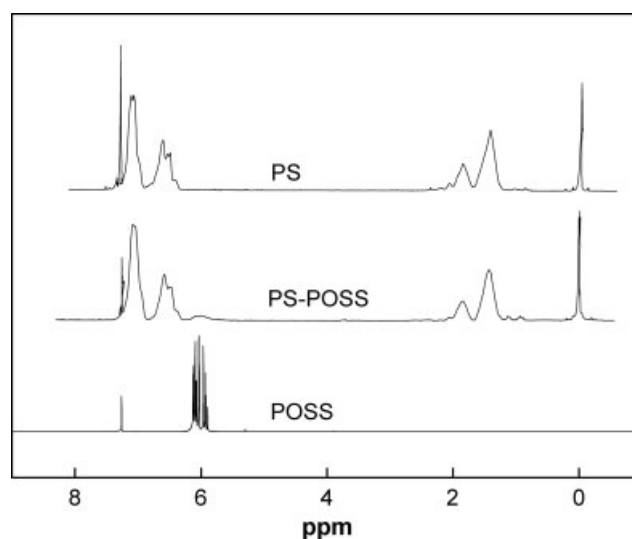

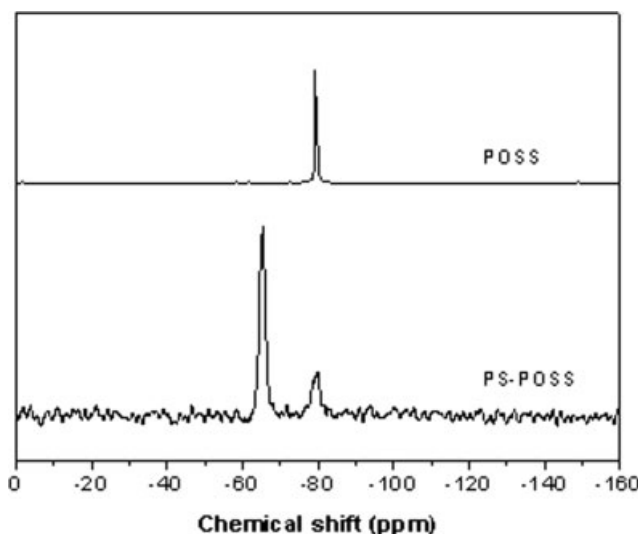**Figure 3** ^{1}H NMR spectra of pure POSS, PS, and PS–POSS nanocomposite.

Figure 4 ^{29}Si NMR spectra of pure POSS and PS–POSS with POSS content 2.21% (Table I. No. 6).

ports the result of ^{1}H NMR analysis. By calculating the peak area ratio, we estimate that about 5–8 vinyl groups on each POSS cage have been consumed in the copolymerization reaction. This result confirms that the resulting hybrid nanocomposites are not linear molecules but possibly star-shaped or network ones.

In principle, network structure should be formed during the copolymerization of styrene and multifunctional octavinyl-POSS. When we compare the reactivities between the styrene and POSS free radicals initiated by the AIBN, however, we think the latter is much weaker simply because of strong spatial hindrance from the bulky POSS, which leads to its low polymerization activity. This result is supported by our previous work.[11,12] As a result, during the polymerization, the styrene would first be initiated and begin to form polystyrene radicals. When these propagating radicals come into contact with POSS free radicals, the termination reactions occur, generating star or linear copolymers rather than network ones. To support our presumption, we tested the solubility of the resultant nanocomposites in a number of solvents such as CHCl$_3$, THF, dioxane and so on. It turned out that these nanocomposites could dissolve in some of the common solvents. This fact convinces us that the synthesized hybrid nanocomposites may mainly consist of star or linear structures rather than of network structures since network polymers are hardly soluble in any solvents. To further study the polymer structure, we treated our products with HF acid to dissolve the POSS cores and leave behind PS chains, and then used GPC to determine the molecular weight distribution of the PS chains. We found that most PS chains were of low polymerization degrees with molecular weights around 1000–2000,

and only 10–20% of the chains were about 3000–4000 in molecular weight. It may indicates that most of the PS chains were the side chains of the POSS cages, and only small amount of them were the linking chains between POSS cages. On the basis of the calculation of the POSS contents in PS–POSS copolymers, we found that when POSS content was low (less than 0.37 mol %), there were only 1–2 POSS in one PS–POSS copolymer, indicating that these PS–POSS copolymers may have star or linear structure. When POSS content was higher (more than 0.37 mol %), there were 2–3 POSS in one PS–POSS, showing that PS–POSS copolymers may have linear or very low cross-linking structures. These results account for the good solubility of hybrid copolymers.

Thermal properties of nanocomposites

Figure 5 shows the DSC thermograms of various PS–POSS hybrid nanocomposites, and the PS homopolymer as well. We see that the T_g's of PS–POSS nanocomposites show a trend of increase with the increase of the POSS content in the nanocomposites, i.e. the T_g's of the nanocomposites increase gradually with the increase of POSS contents and all T_g's are higher than that of PS homopolymer. For example, the PS–POSS hybrid nanocomposite with 0.08 mol % of POSS (PS–POSS0.08) holds a T_g at 94.5°C, which is higher than 92.4°C, T_g of the PS homopolymer. When the molar content of POSS in the nanocomposite increases to 2.21%, the T_g reaches as high as 107.4°C, which is 12.9°C higher than the T_g of the PS homopolymer.

As is known, the T_g of a polymer is primarily related to the structure of the polymer itself. Our previous analyses indicate that the synthesized nanocomposites possess star or low cross-linking
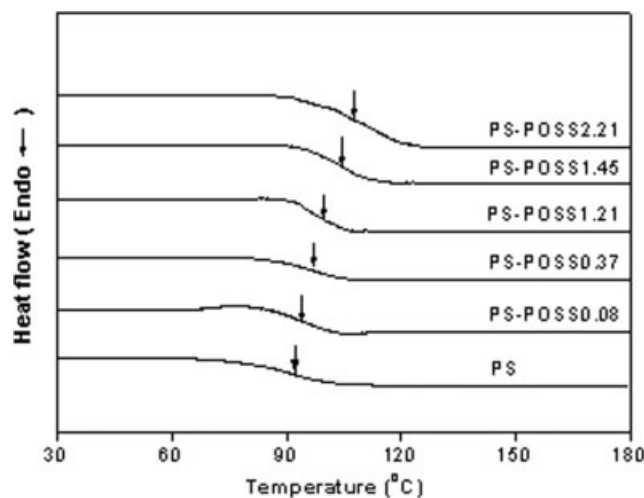

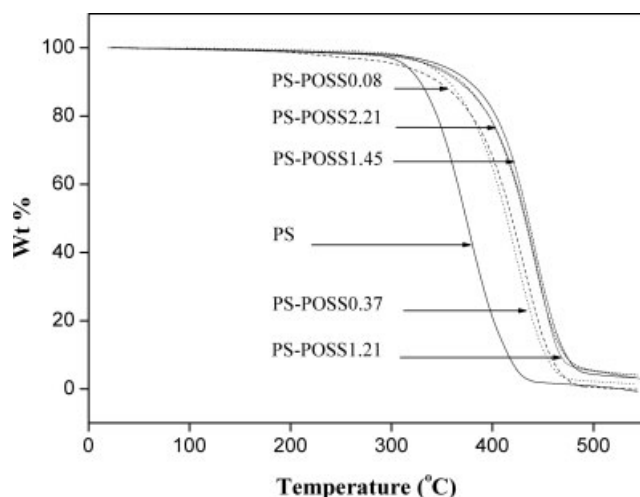**Figure 5** DSC thermograms of pure PS and PS–POSS nanocomposites.

Figure 6 TGA thermograms of pure PS and PS–POSS nanocomposites.

CONCLUSIONS

The well-defined nanosize polyhedral oligomeric silsesquioxane (POSS) was incorporated into the polystyrene by common free radical polymerization to form PS–POSS hybrid nanocomposites. The structures of the PS–POSS hybrid nanocomposites were well characterized by FTIR, ^{1}H NMR, and ^{29}Si NMR, which proved that the resultant nanocomposites were of star and low cross-linking structures. The thermal properties of the PS–POSS hybrid nanocomposites were studied by the DSC and TGA techniques. The results show that both T_g and decomposition temperature of the nanocomposites increases with the POSS content. The remarkable increase of the thermal properties of polymeric materials was mainly due to the structure of the nanocomposites. The nanosize effect of POSS cores also contribute to the improvement of thermal properties.

structures. In these nanocomposites, POSS macromonomers behave as joint points for all the PS chains, and thus restrict the free motion of chain segments, leading to the T_g enhancement. It is obvious that more POSS cores mean more limitation to the PS chains, accounting for the T_g enhancement with the increase of POSS content.

In addition to the structure contribution, we think the nanosize effect of POSS cores is another reason for the reinforcement of T_g. Obviously, there exists an interaction between POSS cores and PS chains since POSS cubes are well-defined nanosize particles and well dispersed in the polymeric system, providing a positive contribution to the T_g increase of the PS–POSS nanocomposites. The similar interaction has been well discussed in our previous research for PAS–POSS nanocomposites.[36]

Figure 6 shows the TGA thermograms of various PS–POSS hybrid nanocomposites and pure PS. The temperatures of 5% weight loss (T_{dec}) and the char yield are recorded in Table I. The PS homopolymer has a T_{dec} at 313.2°C, and has no remnant when the temperature reaches 550°C under N_2. When very small amount of POSS (less than 0.08 mol %) is incorporated into PS, the PS–POSS0.08 showed a T_{dec} at 307.5°C, 5.7°C lower than that of PS homopolymer. For PS–POSS nanocomposites with POSS contents higher than 0.08 mol %, the T_{dec} and char yield increases with the increase of POSS contents. For example, PS–POSS0.37 (POSS content is 0.37 mol %) has a T_{dec} at 334.9°C, 21.7°C higher than pure PS, and no char yield at 550°C. While PS–POSS2.21 has a T_{dec} at 348.1°C, 34.9°C higher than pure PS, and 4% char yield at 550°C. This fact confirms that the incorporation of POSS into polymeric system is a good way to improve the thermal stability of polymeric materials.

References

1. Giannelis, E. P. Adv Mater 1996, 8, 29.
2. Kojima, Y.; Usuki, A.; Kawasumi, M.; Okada, A.; Kurauchi, T.; Kamigaito, O. J Polym Sci Part A: Polym Chem 1993, 31, 983.
3. Novak, B. M. Adv Mater 1993, 5, 422.
4. Pinnavaia, T. J.; Beal, G. W. Polymer Clay Nanocomposites; Wiley: New York, 2001.
5. Schmidt, H. Polymer Based Molecular Composites; Materials Research Society: Pittsburgh, PA, 1990.
6. Baney, R. H.; Itoh, M.; Sakakibara, A.; Suzuki, T. Chem Rev 1995, 95, 1409.
7. Haddad, T. S.; Lichtenhan, J. D. Macromolecules 1996, 29, 7302.
8. Lichtenhan, J. D.; Otonari, Y. A.; Carri, M. J. Macromolecules 1995, 28, 8435.
9. Pyun, J.; Matyjaszewski, K. Macromolecules 2000, 33, 217.
10. Mather, P. T.; Jeon, H. G.; Romo-Uribe, A.; Haddad, T. S.; Lichtenhan, J. D. Macromolecules 1999, 32, 1194.
11. Xu, H. Y.; Kuo, S. W.; Lee, J. S.; Chang, F. C. Polymer 2002, 43, 5117.
12. Xu, H. Y.; Kuo, S. W.; Huang, C. F.; Chang, F. C. J Appl Polym Sci 2004, 91, 2208.
13. Zheng, L.; Farris, R. J.; Coughlin, E. B. Macromolecules 2001, 34, 8034.
14. Coughlin, E. B.; Farris, R. J.; Zheng, L. J Polym Sci Part A: Polym Chem 2001, 39, 2920.
15. Lee, A.; Lichtenhan, J. D. Macromolecules 1998, 31, 4970.
16. Coughlin, E. B.; Farris, R. J.; Zheng, L. Polym Prepr (Am Chem Soc Div Polym Chem) 2001, 42, 885.
17. Fu, B. X.; Zhang, W.; Hsiao, B. S.; Johansson, G.; Sauer, B. B.; Phillips, S.; Balski, R.; Rafailovich, M.; Sokolov, J. Polym Prepr 2000, 41, 587.
18. Fu, B. X.; Hsiao, B. S.; Pagola, S.; Stephens, P.; White, H.; Rafailovich, M.; Sokolov, J.; Mather, P. T.; Jeon, H. G.; Phillips, S.; Lichtenhan, J.; Schwab, J. Polymer 2001, 42, 599.
19. Xu, H. Y.; Kuo, S. W.; Huang, C. F.; Chang, F. C. J Polym Res 2002, 9, 239.
20. Lichtenhan, J. D.; Vu, N. Q.; Carter, J. A. Macromolecules 1993, 26, 2141.
21. Mantz, R. A.; Jones, P. F.; Chaffee, K. P.; Lichtenhan, J. D.; Gilman, J. W. Chem Mater 1996, 8, 1250.
22. Mayadunne, R. T. A.; Jeffery, J.; Moad, G.; Rizzardo, E. Macromolecules 2003, 5, 1505.

23. Zheng, G. H.; Pan, C. Y. Polymer 2005, 8, 2802.
24. Deng, G.; Chen, Y. Macromolecules 2004, 1, 18.
25. Zhao, Y. L.; Chen, Y. M. Chen, C. F.; Xi, F. Polymer 2005, 15, 5808.
26. Huang, C. F.; Lee, H. F.; Kuo, S. W.; Xu, H. Y.; Chang, F. C. Polymer 2004, 7, 2261.
27. Zhang, C. X.; Laine, R. M. J Organometal Chem 1996, 521, 199.
28. Lucke, S.; Stoppek-Langner, K.; Kuchinke, J.; Krebs, B. J Organometal Chem 1999, 584, 11.
29. Fasce, D. P.; Williams, R. J. J.; Mechin, F.; Pascault, J. P.; Liauro, M. F.; Petiaud, R. Macromolecules 1999, 32, 4757.

30. Fasce, D. P.; Williams, R. J. J.; Balsells, R. E.; Ishikawa, Y.; Nonami, H. Macromolecules 2001, 34, 3534.
31. Costa, R. O. R.; Vasconcelos, W. L. Macromolecules 2001, 34, 5398.
32. Tamaki, R.; Tanaka, Y.; Asuncion, M. Z.; Choi, J.; Laine, R. M. J Am Chem Sci 2001, 123, 12416.
33. Ni, Y.; Zheng S. X. Chem Mater 2004, 16, 5141.
34. Harrison, P. G.; Hall, C.; Kannengiesser, R. Main Group Met Chem 1997, 20, 515.
35. Xu, H. Y.; Kuo, S. W.; Lee, J. S.; Chang, F. C. Macromolecules 2002, 35, 8788.
36. Xu, H. Y.; Yang, B. H.; Wang, J. F.; Guang, S. Y.; Li, C. Macromolecules 2005, 38, 10455.